

## Polarization Shaping for Unidirectional Rotational Motion of Molecules

G. Karras, M. Ndong, E. Hertz, D. Sugny, F. Billard, B. Lavorel, and O. Faucher  
*Laboratoire Interdisciplinaire CARNOT de Bourgogne, UMR 6303 CNRS-Université de Bourgogne,  
BP 47870, 21078 Dijon, France*

(Received 12 September 2014; published 10 March 2015)

Control of the orientation of the angular momentum of linear molecules is demonstrated by means of laser polarization shaping. For this purpose, we combine two orthogonally polarized and partially time-overlapped femtosecond laser pulses so as to produce a spinning linear polarization which in turn induces unidirectional rotation of  $N_2$  molecules. The evolution of the rotational response is probed by a third laser beam that can be either linearly or circularly polarized. The physical observable is the frequency shift imparted to the probe beam as a manifestation of the angular Doppler effect. Our experimental results are confirmed by theoretical computations, which allow one to gain a deep physical insight into the laser-molecule interaction.

DOI: 10.1103/PhysRevLett.114.103001

PACS numbers: 37.10.Vz, 42.50.Hz, 42.65.Re

With the rapid advent of technology in the last 50 years, scientists were given the opportunity to control the motion of the basic constituents of matter. This dream became a reality after many attempts in this direction. In the case of the control of molecular rotational dynamics, several schemes have been proposed in order to obtain ensembles with as high an anisotropy on the distribution of the molecular axes as possible. The motivation for these stemmed both from fundamental interests and the thorough understanding of the laser-molecule interaction, but also from any potential applications that might emerge. Electric fields, especially the ones of the laser pulses, proved to be the ideal candidates to reach this promising goal (see for example [1] or the more recent [2] and the references therein). Laser induced nonadiabatic molecular alignment was experimentally demonstrated more than 10 years ago [3], and shortly after, degenerate (multi-) pulse excitation schemes were employed for its optimization [4]. Making a step towards full control of the rotational motion, several works reported on the orientation of the molecular axis [5–7] while a method suggested for inducing orientation of the molecular angular momentum [8] was implemented by Kitano *et al.* [9]. This primary result on the control of the angular momentum dynamics has initiated an intense research activity in the last few years both from the theoretical [8,10–12] and experimental [13–18] aspects. In this framework, recent studies have focused on planar alignment, i.e., the confinement of the molecular axis in a plane [11,13], and on molecular rotation in a preferential direction [16,17]. Different control techniques have been applied in order to produce these dynamics, such as a sequence of two short laser pulses, properly delayed and polarized at  $45^\circ$  with respect to each other [9], a chiral train of ultrashort pulses [15], and the optical molecular centrifuge [19–21]. We point out that such dynamics are expected to have a deep impact for the generation of

superrotors [14], spectroscopic measurements [21], and the formation of macroscopic structures such as gas phase molecular vortices [22].

On the same grounds with these latter works, we experimentally demonstrate the induction of angular momentum orientation (AMO) in  $N_2$  molecules under ambient conditions. For this purpose, we implement a control strategy based on polarization shaping [23]. Even though the field polarization is a critical parameter in control of molecular dynamics, polarization shaping has been under exploited so far [14,19]. AMO appears to be an ideal benchmark problem to test the efficiency of polarization control techniques. In this Letter, we propose a simple polarization shaping scheme enabling AMO and, therefore, unidirectional molecular rotation (UDR). Moreover, using optimization studies, we show that AMO can be significantly increased by using more elaborate shaping.

In order to detect the induced UDR, we used the angular Doppler effect as demonstrated in [16,17]. The angular Doppler effect is an optical effect occurring when circularly polarized (CP) light, with angular frequency  $\omega$ , interacts with anisotropic rotating bodies and manifests itself by the shift of  $\omega$ . For a body rotating at an angular velocity  $\Omega$ , the output field consists of two components: one of the same frequency and polarization as the incident field, and a second CP component of opposite handedness and frequency shifted by  $\Delta\omega = \pm 2\Omega$ . The sign depends on the helicity of the wave with respect to the sense of molecular rotation. The frequency is downshifted (upshifted) for an incident CP field rotating in the same (opposite) sense as the molecule. The angular doppler effect is well suited for the characterization of molecular spinning under consideration. Spectral analysis of the reversed handedness CP field, that can be isolated by means of a circular analyzer, indeed, provides a signature of UDR along with the speed and the direction of the molecular rotation.

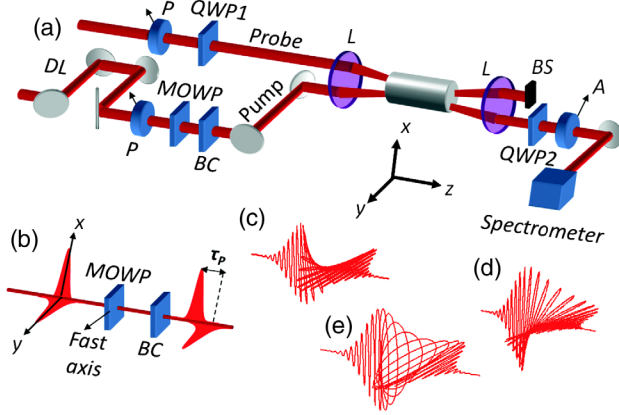


FIG. 1 (color online). (a) Experimental setup (see text). (b) Polarization shaping setup (see text). (c) and (d) Illustration of the electric field for phase  $\varphi_p = 0$  and  $\pi [2\pi]$ , producing a linear “twisted” polarization in the clockwise and counterclockwise direction, respectively. (e) The same for intermediate phase  $\varphi_p$  leading to an elliptical polarization in the overlapping region of the two pulses.

The experimental setup is displayed in Fig. 1(a). Pump and probe beam are produced from a Ti:sapphire chirped pulse amplifier that delivers pulses of 100 fs duration, centered around 800 nm, at 1 kHz repetition rate. The pump-probe pulse delay  $\tau$  is adjusted via a motorized delay line (DL). The two beams are crossed at a small angle and focused inside a static cell filled with  $N_2$  molecules under ambient conditions. According to the measurements we want to perform and the information we need to access, the probe beam can be either circularly or linearly polarized. Circular polarization is achieved by placing a circular polarizer [polarizer ( $P$ ) and quarter wave plate (QWP1)] prior to the focusing lens ( $L$ ). In this case, a circular analyzer [QWP2 and analyzer ( $A$ )] allows measurement of the scattered signal and, specifically, of the component of the CP field having experienced inversion in its handedness. The beam is then sent to a spectrometer in order to record its spectral characteristics. When the probe beam is linearly polarized, both QWPs are removed. In principle, the Doppler effect can also be measured with linear polarization [16]. Nevertheless, in this Letter, we will show that this configuration can lead to misleading conclusions for the particular case of UDR.

In order to induce unidirectional rotational motion to the molecules, we shape the polarization of the pump pulse by introducing a multiple order wave plate (MOWP) in conjunction with a Berek compensator (BC) on the pump beam path. As shown in Fig. 1(b), the pump is initially polarized at  $45^\circ$  with respect to the fast and slow axes of the MOWP. After propagation through the latter, the different group velocity experienced by the field components produces two time-delayed and cross-polarized pulses. The time delay is set to  $\tau_p \approx 145$  fs ensuring a significant overlap between the two pulses. The leading (trailing) edge

of the pulse is polarized along the  $y$  ( $x$ ) axis, while the polarization in the overlapping region is determined by the relative phase  $\varphi_p$  between the  $y$ - and  $x$ -field component. For  $\varphi_p = 0 [2\pi]$ , the polarization remains linear but “twisted” from  $y$  to  $x$  due to the continuous variation of the relative field amplitude between these axes. As a result, the pump pulse exhibits a spinning linear polarization in the clockwise direction as shown in Fig. 1(c). For  $\varphi_p = \pi [2\pi]$ , the polarization is twisted in the counterclockwise direction [Fig. 1(d)] while intermediate phases produce an elliptical polarization in the middle of the pulse [Fig. 1(e)]. The phase  $\varphi_p$  is finely adjusted with the BC by observing spectral fringes (see the Supplemental Material [24] for details). It is worth mentioning that, instead of a fixed delay, a tunable and phase stabilized delay could also be produced by means of a Pockels cell conferring a great flexibility on the present method with respect to the molecular system.

Such a polarization shaping is a valuable tool for controlling the rotational motion of molecules and particularly for the production of UDR. In a classical picture, a pulse with a linear polarization that continuously rotates at a speed in the THz regime, i.e., at the same angular velocity as the molecules, is in principle suitable for inducing molecular spinning. This qualitative argument is supported by the following numerical study. Initially, we consider the  $N_2$  molecules in their ground vibronic state, subjected to two nonresonant linearly polarized laser fields, along the  $x$  and  $y$  directions. In this case, the pump field  $\vec{\mathcal{E}}_p$  can be written

$$\vec{\mathcal{E}}_p = E_x(t - \tau_p) \cos(\omega t - \varphi_p) \vec{e}_x + E_y(t) \cos(\omega t) \vec{e}_y, \quad (1)$$

where  $\omega$  is the angular frequency,  $\varphi_p$  is the relative phase defined as  $\varphi_p = \omega \tau_p + \varphi_0$ , with  $\tau_p$  the relative time delay and  $\varphi_0$  the additional phase difference between the two polarization directions induced by the Berek compensator. Within the rigid rotor and high-frequency approximation, it can be shown that the dynamics are generated through the Liouville–von Neumann equation by the time-dependent Hamiltonian

$$H(t) = H_0 + H_x + H_y + H_{xy}. \quad (2)$$

Here,  $H_0$  is the field-free Hamiltonian, which governs the molecular rotational dynamics and the three other terms describe the coupling of the molecule to the external field. They read

$$\begin{aligned} H_0 &= BJ^2 - DJ^4, \\ H_{xy} &= -\frac{1}{2} E_x(t - \tau_p) E_y(t) \Delta \alpha \cos(\varphi_p) \cos \theta_x \cos \theta_y, \\ H_x &= -\frac{1}{4} E_x^2(t - \tau_p) (\alpha_\perp + \Delta \alpha \cos^2 \theta_x), \\ H_y &= -\frac{1}{4} E_y^2(t) (\alpha_\perp + \Delta \alpha \cos^2 \theta_y), \end{aligned} \quad (3)$$

with  $B$  and  $D$  the rotational constants,  $J^2$  the angular momentum operator,  $\Delta\alpha = \alpha_{\parallel} - \alpha_{\perp}$  the difference between the parallel and perpendicular components of the polarizability tensor, and  $\theta_i$  the angle of the molecular axis with respect to the  $i$  axis. The numerical values of the different molecular parameters used in the simulations are, respectively,  $B = 1.989 \text{ cm}^{-1}$ ,  $D = 5.71 \times 10^{-6} \text{ cm}^{-1}$ ,  $\alpha_{\parallel} = 14.82 \text{ a.u.}$ , and  $\alpha_{\perp} = 10.2 \text{ a.u.}$

Let us denote by  $\{|j, m\rangle\}$  the spherical Harmonic basis of the Hilbert space. For  $m > 0$ , we introduce the even and odd symmetrized states  $|j, m\rangle_{\pm}$  such that  $|j, m\rangle_{\pm} = (|j, m\rangle \pm |j, -m\rangle)/\sqrt{2}$  and  $|j, 0\rangle_{+} = |j, 0\rangle$ . A superposition of only  $|j, m\rangle_{+}$  (or  $|j, m\rangle_{-}$ ) states does not lead to any AMO. On the contrary, a wave packet with components over both  $|j, m\rangle_{+}$  and  $|j, m\rangle_{-}$  states gives AMO with a maximum achieved for a balanced distribution between  $|j, m\rangle_{+}$  and  $|j, m\rangle_{-}$  states. The initial thermal equilibrium state is a density matrix which can be expressed in terms of the  $|j, m\rangle_{+}$  states. A careful inspection of the different matrix coupling elements shows that the Hamiltonians  $H_x$  and  $H_y$  only couple together the even and odd states, while the operator  $\cos\theta_x \cos\theta_y$  can induce transitions from  $|j, m\rangle_{\pm}$  to  $|j, m\rangle_{\mp}$  [11]. In the absence of the  $H_{xy}$  term, i.e., for  $\varphi_p = \pi/2$ , no asymmetry in the positive and negative  $m$  values can be produced by the control field. The system is, thus, composed of two perfectly symmetric ensembles of molecules with opposite UDR. This theoretical argument shows the strong dependence on  $\varphi_p$  of the UDR, which is maximized when the phase takes the values 0 and  $\pi$ .

In order to establish a clear relationship to the experimental data, we model the angular Doppler effect and the frequency shift imparted to a CP electric field through the interaction with an anisotropic rotating body. In the case under concern, the electric field  $\vec{E}$  of the probe beam after QWP1 is CP, and thus, by using complex notation, its coordinates in the  $(x, y)$  plane are, up to a scaling factor,  $[E_0(t)e^{i\omega t}, E_0(t)e^{i(\omega t - \pi/2)}]$ , where  $E_0(t) = E_0 \exp[-(t - \tau)^2/\sigma^2]$  with  $\tau$  the pump-probe delay.

Because of its relatively low intensity, we can deduce the resulted electric field after the interaction of the probe pulse with the molecular sample from the expression of the dipole moment  $\vec{\mu} = 1/2\vec{\alpha} \cdot \vec{E}_p$  induced by  $\vec{E}_p$ . Since  $\text{N}_2$  has no permanent dipole moment, we get at first order a field  $\vec{E}$  with coordinates  $E_0/2e^{i\omega t}(\alpha_{11} + \alpha_{12}e^{-i\pi/2}, \alpha_{21} + \alpha_{22}e^{-i\pi/2})$ , where the  $\alpha_{ij}$  are the components of the polarizability tensor in the laboratory frame. After QWP2 and the analyzer, we deduce that the amplitude of the electric field signal is of the form

$$E_S(t) \simeq E_0(t)\Delta\alpha e^{i\omega t}\sin^2\theta e^{-2i\varphi}, \quad (4)$$

where  $(\theta, \varphi)$  are the polar coordinates of the molecular axis in the laboratory frame. In a simplified picture, the Doppler

shift of the probe beam can be easily understood as follows. In the ideal unidirectional motion, we have  $\theta \simeq \pi/2$  [the molecular axis is confined in the  $(x, y)$  plane] and  $\varphi = \pm\Omega t$  according to the rotation sense. Thus, from Eq. (4), we obtain that  $E_S(t) \simeq e^{i(\omega \pm 2\Omega)t}$ , and consequently, a shift  $\Delta\omega = \pm 2\Omega$  towards lower or higher frequencies is imparted to the initially measured spectrum. In a realistic situation, since  $\sin^2\theta$  is a time dependent function, the spectrum also exhibits a broadening.

A first insight into the quantum molecular dynamics is given by the evolution of the angular distribution of the  $\text{N}_2$  molecule after the switch off of the control field. These dynamics are depicted in Fig. 2 for three successive times around the half rotational period. While a UDR cannot be clearly observed on the three-dimensional picture due to the thermal averaging of the dynamics, two-dimensional traces in the  $(x, y)$  plane provide an unambiguous evidence of its presence.

Figure 3 shows the angular Doppler measurements performed around the half rotational period with a right CP probe pulse. Figures 3(a) and 3(b) correspond to molecules excited with a field of spinning linear polarization in the clockwise ( $\varphi_p = 0$ ) and counterclockwise ( $\varphi_p = \pi$ ) direction, respectively. The measurements reveal the expected redshift (blueshift) for molecules rotating in the same (opposite) direction with respect to the handedness of the CP probe field, in excellent agreement with the theoretical model. The significance of the phase  $\varphi_p$  in the induction of AMO is manifested in Fig. 3(c) where we

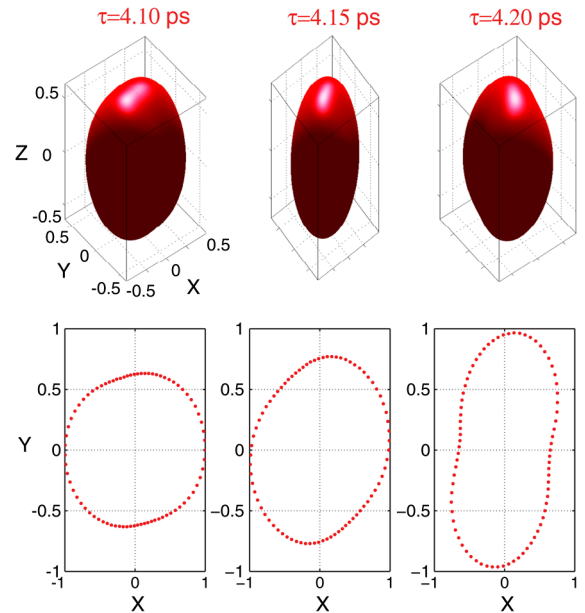


FIG. 2 (color online). (Top panels) Angular distributions of the rotational axis of  $\text{N}_2$  calculated at different times within the revival at the half rotational period. (Bottom panels) Traces of the angular distribution projected to the  $(x, y)$  plane characterizing the counterclockwise direction of the UDR.

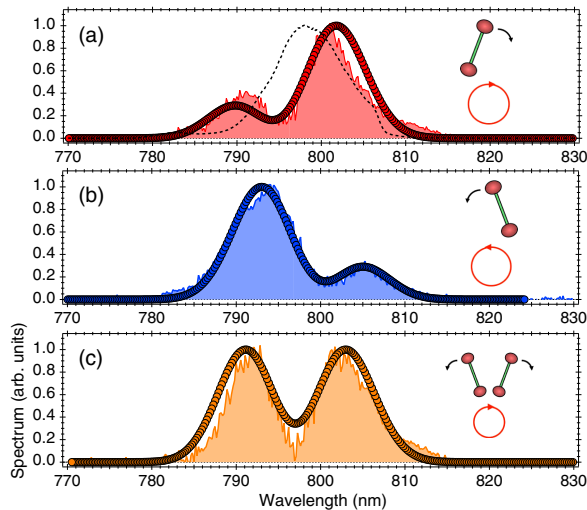


FIG. 3 (color online). Normalized spectra of the circularly polarized probe beam recorded at a pump-probe time delay  $\tau = 4.2$  ps for a shaped pulse with phase (a)  $\varphi_p = 0$  (red-filled area), (b)  $\varphi_p = \pi$  (blue-filled area), and (c)  $\varphi_p = \pi/2$  (orange-filled area). The respective theoretical spectra are represented with solid circles. The input probe spectrum is shown in (a) with a black dashed line.

present the profile of the recorded spectrum at the same conditions as the above for  $\varphi_p = \pi/2$ . In this case, the shaped pump pulse contains a CP part in the middle of the pulse envelope which wipes out the molecular spinning as explained before. The spectrum is then symmetric with respect to the central angular frequency of the laser without any shift in a preferred direction.

The angular Doppler effect can also be observed, in principle, using a linearly polarized probe pulse. Since a linear polarization can be regarded as the sum of two counter-rotating CP fields, a spectral shift will be imparted to the two components, with opposite signs, resulting in the splitting of the initial spectrum into two equal parts. Observing a splitting, therefore, should be a signature of UDR although the sense of molecular rotation remains unknown. The use of a linear polarization is practically convenient since the quality of the attained extinction is significantly better than the one obtained with a circular polarizer and analyzer. In Fig. 4, the corresponding experimental results for  $\varphi_p = 0$  show, as expected, that the probe spectrum is split. However, for  $\varphi_p = \pi/2$ , we see, from Fig. 4, that the splitting remains while no UDR is imparted by the pump pulse. This behavior is purely a quantum mechanical effect which can be understood by considering that a pulse shaping with a  $\pi/2$  phase will result in two sets of molecules, equally populated, rotating in opposite directions. Hence, each counter rotating CP field of the linearly polarized probe will interact with both sets and will then be split. The splitting observed for a CP polarization in Fig. 3(c) with  $\pi/2$  corroborates this claim. As a result, measurement performed with a linearly

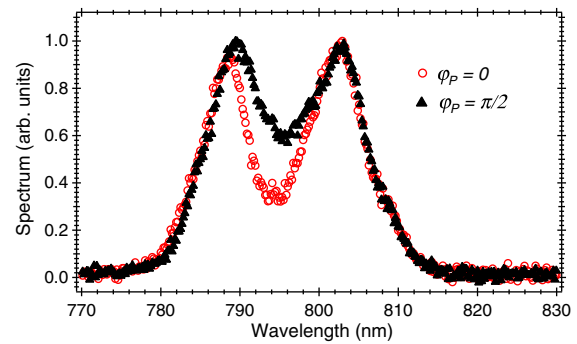


FIG. 4 (color online). Normalized spectrum of the linearly polarized probe beam recorded at a pump-probe time delay  $\tau = 4.2$  ps for  $\varphi_p = 0$  (red circles) and  $\varphi_p = \pi/2$  (black triangles).

polarized probe field cannot *a priori* attest to the presence of UDR.

The comparison between our polarization shaping technique and the one based on two nonoverlapping linearly polarized pulses at  $45^\circ$  with respect to each other [9] leads to similar results in terms of AMO efficiency, which can be estimated from different observables evaluated in the time or frequency domain. Optimal control theory can be applied to enhance the degree of AMO. The numerical results are presented in the Supplemental Material [24]. We show, in particular, that the optimized field, which could be easily produced by standard experimental pulse shaping techniques, increases the AMO by a factor of 2. Note that the two separate pulses used in Ref. [9] require a long time delay between them (several picoseconds for  $N_2$ ) and are, therefore, hardly compatible with close- or open-loop optimization procedures. Additionally, schemes based on long time delayed pulses are more exposed to collisional dynamics when the measurements are performed in dense gas media. These differences confer a benefit on the present polarization shaping method. Finally, while the optical centrifuge technique appears more efficient for UDR, the production of the effect under field-free conditions is, nevertheless, harder to achieve compared with the present technique and multipulse methods [9,15].

In conclusion, we have proposed a simple control strategy for producing AMO of  $N_2$  molecules at ambient conditions for the temperature and the pressure. Our approach is based on the shaping of the laser polarization, and its efficiency has been experimentally demonstrated by using the angular Doppler effect. Our theoretical model is in a satisfactory agreement with the measurements and, thus, provides further insight to several interesting characteristics of the interaction. Furthermore, by using the technique of optimal control theory, we have numerically shown that AMO can be significantly enhanced by a judicious and nonintuitive shaping of the laser field polarization. As recently shown, molecular superrotors involving unidirectional ultrafast rotation strongly impact collision-induced dissipation mechanisms in gaseous

media [21]. Thus, orientation of rotational angular momentum might provide the useful means for the control over inelastic and reactive collisions. Besides its application to molecular rotational dynamics, our approach paves the way to a systematic use of control techniques in other domains of quantum control where it is also desirable to shape the laser polarization. In addition, the proposed scheme for the induction of AMO could be potentially applied using laser filaments, and in this case, the amplitude of the electric field that could be frequency shifted would be significantly increased.

This work was supported by the Conseil Régional de Bourgogne (PARI Program), the CNRS, the Labex ACTION Program (Contract No. ANR-11-LABX-01-01), and the French National Research Agency (ANR) through the CoConicS Program (Contract No. ANR-13-BS08-0013). D. Sugny acknowledges support from the QUAINT coordination action (EC FET-Open).

- 
- [1] H. Stapelfeldt and T. Seideman, *Rev. Mod. Phys.* **75**, 543 (2003).
- [2] M. Lemeshko, R. V. Krems, J. M. Doyle, and S. Kais, *Mol. Phys.* **111**, 1648 (2013).
- [3] F. Rosca-Pruna and M. J. J. Vrakking, *Phys. Rev. Lett.* **87**, 153902 (2001).
- [4] C. Z. Bisgaard, M. D. Poulsen, E. Peronne, S. S. Viftrup, and H. Stapelfeldt, *Phys. Rev. Lett.* **92**, 173004 (2004).
- [5] S. Fleischer, Y. Zhou, R. W. Field, and K. A. Nelson, *Phys. Rev. Lett.* **107**, 163603 (2011).
- [6] K. Oda, M. Hita, S. Minemoto, and H. Sakai, *Phys. Rev. Lett.* **104**, 213901 (2010).
- [7] S. De, I. Znakovskaya, D. Ray, F. Anis, N. G. Johnson, I. A. Bocharova, M. Magrakvelidze, B. D. Esry, C. L. Cocke, I. V. Litvinyuk, and M. F. Kling, *Phys. Rev. Lett.* **103**, 153002 (2009).
- [8] S. Feischer, Y. Khodorkovsky, Y. Prior, and I. S. Averbukh, *New J. Phys.* **11**, 105039 (2009).
- [9] K. Kitano, H. Hasegawa, and Y. Ohshima, *Phys. Rev. Lett.* **103**, 223002 (2009).
- [10] M. Lapert, S. Guerin, and D. Sugny, *Phys. Rev. A* **83**, 013403 (2011).
- [11] M. Lapert, E. Hertz, S. Guerin, and D. Sugny, *Phys. Rev. A* **80**, 051403 (2009).
- [12] C. Bloomquist, S. Zhdanovich, A. A. Milner, and V. Milner, *Phys. Rev. A* **86**, 063413 (2012).
- [13] M. Z. Hoque, M. Lapert, E. Hertz, F. Billard, D. Sugny, B. Lavorel, and O. Faucher, *Phys. Rev. A* **84**, 013409 (2011).
- [14] A. Korobenko, A. A. Milner, and V. Milner, *Phys. Rev. Lett.* **112**, 113004 (2014).
- [15] S. Zhdanovich, A. A. Milner, C. Bloomquist, J. Floss, I. S. Averbukh, J. W. Hepburn, and V. Milner, *Phys. Rev. Lett.* **107**, 243004 (2011).
- [16] U. Steinitz, Y. Prior, and I. S. Averbukh, *Phys. Rev. Lett.* **112**, 013004 (2014).
- [17] O. Korech, U. Steinitz, R. J. Gordon, I. S. Averbukh, and Y. Prior, *Nat. Photonics* **7**, 711 (2013).
- [18] T. Vieillard, F. Chaussard, F. Billard, D. Sugny, O. Faucher, S. Ivanov, J.-M. Hartmann, C. Boulet, and B. Lavorel, *Phys. Rev. A* **87**, 023409 (2013).
- [19] J. Karczmarek, J. Wright, P. Corkum, and M. Ivanov, *Phys. Rev. Lett.* **82**, 3420 (1999).
- [20] L. Yuan, S. W. Teitelbaum, A. Robinson, and A. S. Mullin, *Proc. Natl. Acad. Sci. U.S.A.* **108**, 6872 (2011).
- [21] A. A. Milner, A. Korobenko, J. W. Hepburn, and V. Milner, *Phys. Rev. Lett.* **113**, 043005 (2014).
- [22] U. Steinitz, Y. Prior, and I. S. Averbukh, *Phys. Rev. Lett.* **109**, 033001 (2012).
- [23] T. Brixner and G. Gerber, *Opt. Lett.* **26**, 557 (2001).
- [24] See Supplemental Material at <http://link.aps.org/supplemental/10.1103/PhysRevLett.114.103001> for the experimental characterization of the field polarization in the middle of the pulse and for a complete description of the optimal control computations with the corresponding results, which includes Refs. [25,26].
- [25] M. Ndong, M. Lapert, C. P. Koch, and D. Sugny, *Phys. Rev. A* **87**, 043416 (2013).
- [26] M. Lapert, R. Tehini, G. Turinici, and D. Sugny, *Phys. Rev. A* **78**, 023408 (2008).